

Molecular mechanisms of precise timing in cell lysis

Anupam Mondal,^{1,2} Hamid Teimouri,^{1,2} and Anatoly B. Kolomeisky^{1,2,3,*}

¹Center for Theoretical Biological Physics, Rice University, Houston, Texas; ²Department of Chemistry, Rice University, Houston, Texas; and ³Department of Chemical and Biomolecular Engineering, Rice University, Houston, Texas

ABSTRACT Many biological systems exhibit precise timing of events, and one of the most known examples is cell lysis, which is a process of breaking bacterial host cells in the virus infection cycle. However, the underlying microscopic picture of precise timing remains not well understood. We present a novel theoretical approach to explain the molecular mechanisms of effectively deterministic dynamics in biological systems. Our hypothesis is based on the idea of stochastic coupling between relevant underlying biophysical and biochemical processes that lead to noise cancellation. To test this hypothesis, we introduced a minimal discrete-state stochastic model to investigate how holin proteins produced by bacteriophages break the inner membranes of gram-negative bacteria. By explicitly solving this model, the dynamic properties of cell lysis are fully evaluated, and theoretical predictions quantitatively agree with available experimental data for both wild-type and holin mutants. It is found that the observed threshold-like behavior is a result of the balance between holin proteins entering the membrane and leaving the membrane during the lysis. Theoretical analysis suggests that the cell lysis achieves precise timing for wild-type species by maximizing the number of holins in the membrane and narrowing their spatial distribution. In contrast, for mutated species, these conditions are not satisfied. Our theoretical approach presents a possible molecular picture of precise dynamic regulation in intrinsically random biological processes.

SIGNIFICANCE Biological systems show remarkable precision in the timing of their events, which might be surprising since the underlying biochemical processes are random. We propose a new theoretical approach that might explain the molecular mechanisms of these dynamic phenomena. It is based on the idea of coupling between several stochastic processes that might cancel the noise. To test this, we developed a minimal model to analyze the precise dynamics of holin proteins, produced by bacteriophages, that break bacterial cellular membranes. Our theoretical analysis, which agrees well with experimental observations, suggests that precise timing can be achieved by providing the maximal number of holin proteins in the membrane while keeping their distribution narrow.

INTRODUCTION

A large number of biological processes exhibit remarkable precision in the timing of cellular events that they regulate, including cell differentiation (1–3), bacterial sporulation (4,5), cell cycle control (6–8), biological development (9,10), gene expression (11–13), cell size regulation (14–16), and many others. In most of these systems, it is observed that the accumulation of some regulatory proteins reaches threshold concentrations, after which the specific events start. These observations are surprising since all biological systems rely on a very large number of intrinsically random biochemical and biophysical processes that are also taking place in a randomly fluctuating environment.

Although significant progress in our understanding of noise in biological systems has been achieved (17–22), the molecular mechanisms of precise timing remain not well clarified.

One of the most known examples of precise timing is cell lysis by λ bacteriophage viruses (23). After infecting the bacterial cell and choosing a viral reproduction pathway (24), the virus stimulates the host to produce holins, small 105-aa-length membrane proteins with three transmembrane domains encoded by the *S* gene of phage λ (25). During the late viral reproduction phase, holin proteins start to progressively accumulate in the inner membrane (see Fig. 1 A) initially, without any visible impact on membrane integrity or structure (26). Experiments confirm that this accumulation also does not affect vital cellular functions (26). Then, suddenly, at a time when the holin concentration reaches a specific threshold, an abrupt transition of proteins into the formation of irregular lesions (>300 nm) within the membrane occurs (27). These holes serve as channels for the

Submitted February 7, 2024, and accepted for publication July 2, 2024.

*Correspondence: tolya@rice.edu

Editor: Jing Chen.

<https://doi.org/10.1016/j.bpj.2024.07.008>

© 2024 Biophysical Society. Published by Elsevier Inc.

All rights are reserved, including those for text and data mining, AI training, and similar technologies.

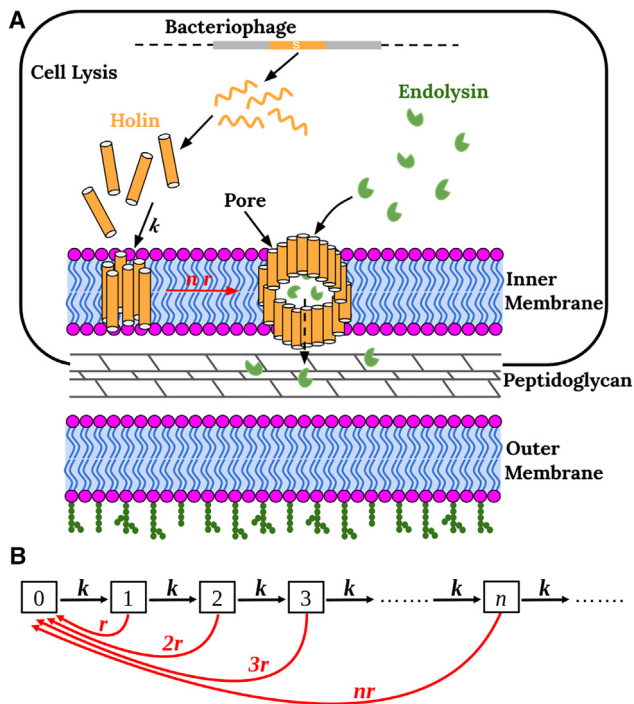


FIGURE 1 (A) Schematic view of the gram-negative bacterial cell infected by phage viruses. The produced holin proteins diffuse into the inner membrane, triggering the creation of holes in the membrane. Endolysin enzymes, also produced by the phage, move through these holes and attack the peptidoglycan cell walls. (B) A minimal discrete-state stochastic model of cell lysis. States correspond to the number of holins in the membrane. The rate of accumulating a holin protein is k , and the rate constant of lysis is r .

release of the phage endolysin proteins from the cytoplasm (see Fig. 1 A), stimulating the rapid destruction of the cell wall within a few seconds (26). In phages of gram-negative hosts, an additional phase in the lysis process occurs, which entails the synthesis of so-called spanin proteins that fuse the inner and outer membranes (28–32), completing the opening of the bacterial cells for virions to come out and infect other bacterial cells.

To understand the mechanisms of precise timing in biological systems, it is convenient to consider cell lysis triggered by holin proteins. This is because this process has been well studied using a variety of experimental methods that provided a large amount of quantitative information (26,27,32–34). It has been found that adding molecules that lead to partial membrane depolarization, so-called “energy poisons”, produces premature triggering of holin proteins at concentrations lower than typical threshold values (26). In addition, experiments showed that cell lysis dynamics are strongly affected by mutations in various regions of the holin sequences, with particular sensitivity in the three transmembrane domains (35–39). In a recent study, site-directed mutagenesis experiments creating a large spectrum of mutations in the S105 holin allele produced diverse holin gene variants, each introducing one or two amino acid substitutions. Quantitative measure-

ments of lysis dynamics for these variants, assessed at the individual cell level, displayed a surprising nonmonotonic behavior, with the wild-type (WT) λ phages exhibiting a minimum in lysis timing noise (40), while all mutants showed higher variations in cell lysis times. In addition, WT species did not exhibit the fastest lysis times. Surprisingly, several mutant species were able to break cell membranes faster than WT species.

Multiple theoretical attempts to understand the mechanisms of cell lysis timing have been proposed, exploring different approaches (13,17,40,41–44). It was mainly viewed as an example of stochastic timing events stimulated by different gene expression levels. The first-passage approach has been utilized to mimic the reaching of protein thresholds in experimental systems (13,17). While these theoretical investigations were able to describe many aspects of cell lysis dynamics, the main problem with these studies is that the most important fundamental questions, such as the microscopic origin of thresholds and precise timing, have not been addressed due to the phenomenological nature of these theories (17,41,43). Namely, the thresholds were assumed from the beginning, and then it was not possible to understand the microscopic origin of such behavior. It seems that, currently, there is no quantitative theoretical method that can analyze cell lysis phenomena from a more molecular point of view, connecting underlying biochemical and biophysical molecular processes to macroscopic observations.

In this paper, we propose a new theoretical framework for analyzing precise timing events in biological systems. Our central hypothesis is that such almost deterministic dynamic regulation might be achieved as a result of the coupling of several underlying stochastic processes that lead to effectively threshold-like behavior. The idea here is that such coupling might cancel the noise from each of the processes. To test our hypothesis, we specifically investigate the microscopic origin of precise timing in cell lysis by λ bacteriophages by considering a minimal stochastic model that can be explicitly solved. This allows us to quantitatively describe experimental observations, explaining the appearance of thresholds and providing molecular arguments to clarify why the cell lysis dynamics is so precise.

MATERIALS AND METHODS

Theoretical model

To investigate the molecular mechanisms of cell lysis dynamics, we propose a minimal discrete-state stochastic model that accounts for the most relevant processes, as illustrated in Fig. 1 B. The system can be characterized by a set of discrete states n , where n is the number of holin proteins in the membrane. This number can increase by one with an effective holin accumulation rate k (Fig. 1 B), which combines several processes, such as the diffusion of protein molecules to the cytoplasmic membrane, entering the membrane, and spreading within the membrane. Note here

that our model does not assume that the holin proteins degrade, in agreement with experimental observations pointing out that holin proteins are long lived and do not undergo degradation over relevant timescales (45,46). From any state of the system, the lysis can happen with a rate constant r (rate per unit protein), which means that the lysis rate from the state n is equal to nr , i.e., proportional to the number of holins already present in the inner membrane, as shown in Fig. 1 B. To explore more realistic biological scenarios, we also considered a power-law dependence in the lysis rate, where the lysis rate is proportional to n^α , with α being the stoichiometric exponent. Detailed calculations for this extended model are provided in the supporting material. Notably, our analysis shows that the power-law dependence does not alter the theoretical predictions for key quantities compared to the scenario that considers linear dependence. Thus, in our current model, we assume the lysis rate is proportional to the number of holins, n .

It is important to note here that our assumption of the overall lysis rate being proportional to the number of proteins already in the membrane is the simplest picture. This seems to be a realistic approximation because it is known that holins aggregate before breaking the membranes, and it is reasonable to view the aggregation as a chemical reaction of the assembly of oligomers from monomers that should be proportional to the number of individual holin proteins. At the same time, if future experiments show a more complex dependence, then the theoretical model can be extended. In addition, in our theoretical framework, reversion back to zero signifies a reset akin to starting a new experimental observation rather than implying the reappearance of the already lysed cells in the system.

The main difference of our approach from other theoretical studies is that we postulate that lysis can happen for any amount of holin proteins in the inner membrane (see Fig. 1 B). However, because of the stochastic coupling with the holin accumulation, the lysis essentially happens with high probability only at a relatively narrow range of protein concentrations in the membrane, as we will see below. This eliminates the necessity to introduce and justify the appearance of the protein thresholds, which is the weakest point in existing phenomenological approaches (17,40,41,43).

To analyze the stochastic model presented in Fig. 1 B, we define $P_n(t)$ ($n = 0, 1, 2, \dots$) as the probability to have n holin proteins in the membrane, i.e., to have the system in the state n at time t . Then, the temporal evolution of such probabilities are governed by a set of forward master equations,

$$\frac{dP_0(t)}{dt} = \sum_{n=1}^{\infty} rnP_n(t) - kP_0(t), \quad (\text{Equation 1})$$

and for $n \neq 0$,

$$\frac{dP_n(t)}{dt} = kP_{n-1}(t) - (k + nr)P_n(t). \quad (\text{Equation 2})$$

In addition, we have the normalization condition,

$$\sum_{n=0}^{\infty} P_n = 1. \quad (\text{Equation 3})$$

While it has not been shown in experiments that the system reaches the steady state, given the fact that the lysis times are large (~ 100 min), the assumption that the system might quickly reach the stationary state is reasonable. Assuming that ($t \rightarrow \infty$), one can calculate the stationary-state distributions P_n of holin proteins in the membrane, as shown in detail in the supporting material, yielding

$$P_n = \frac{x^n}{\prod_{j=1}^n (x + j)} P_0, \quad (\text{Equation 4})$$

where $x = \frac{k}{r}$ is the coupling parameter between holin accumulation and holin removal due to lysis. In addition,

$$P_0 = \frac{1}{\sum_{n=0}^{\infty} \left[\frac{x^n}{\prod_{j=1}^n (x + j)} \right]}, \quad (\text{Equation 5})$$

is the stationary probability of having zero holins in the membrane. This allows us to estimate the average number of holin proteins in the membrane at stationary conditions,

$$\langle n \rangle = \sum_{n=1}^{\infty} nP_n = xP_0. \quad (\text{Equation 6})$$

The results of our calculations are presented in Fig. 2. As one can see, increasing the value of the coupling parameter x makes stationary distributions of holin proteins broader (Fig. 2 A), and the average number of proteins inside the membrane increases (Fig. 2 B), as expected.

To describe the dynamics of cell lysis, we utilize a method of first-passage probabilities (47,48). More specifically, one can define a function $F_n(m, t)$ as the probability density of cell lysis occurring for the first time from the state m (see Fig. S1) at time t if, at $t = 0$, the system started in the state n ($0 \leq n \leq m$). Note that this quantity is different from the probability functions $P_n(t)$, and it has its own normalization condition, $\int_0^{\infty} F_n(m, t) dt = 1$. The temporal evolution of these functions is governed by the backward master equations

$$\frac{dF_n(m, t)}{dt} = kF_{n+1}(m, t) - (k + nr)F_n(m, t) \quad (\text{Equation 7})$$

for $1 \leq n < m$. In addition, at $n = 0$, we have

$$\frac{dF_0(m, t)}{dt} = kF_1(m, t) - kF_0(m, t), \quad (\text{Equation 8})$$

while for $n = m$,

$$\frac{dF_m(m, t)}{dt} = mrF_{cl}(m, t) - (k + mr)F_m(m, t), \quad (\text{Equation 9})$$

where $F_{cl}(m, t)$ is the probability of being found in the state immediately after the cell lysis. So, it is natural to assume that $F_{cl}(m, t) = \delta(t)$. This physically means that if the system is in this state at $t = 0$, then the process of cell lysis is immediately accomplished.

As described in detail in the supporting material, these equations can be solved analytically using Laplace transformations $\tilde{F}_n(m, s) \equiv \int_0^{\infty} e^{-st} F_n(m, t) dt$, producing the distributions of the cell lysis time, which is the quantity that has been experimentally measured (38,40). It can be shown that for realistic values of $x \gg 1$, the probability distribution of lysis times in the Laplace domain is given by

$$\tilde{F}_0(m, s) \simeq \frac{mx^m}{\left(\frac{s}{r} + x\right)^{m+1}}, \quad (\text{Equation 10})$$

which can be easily inverted to obtain the first-passage distribution function of the lysis times,

$$F_0(m, t) = F_0(t) \simeq \frac{k(k t)^m e^{-kt}}{m!}. \quad (\text{Equation 11})$$

The advantage of using Laplace transformations is that all dynamic properties in the system can be explicitly evaluated. For example, the probability for cell lysis to occur in the state m (a so-called splitting probability (47,48)) starting from the state $n = 0$ can be estimated (for large x) as

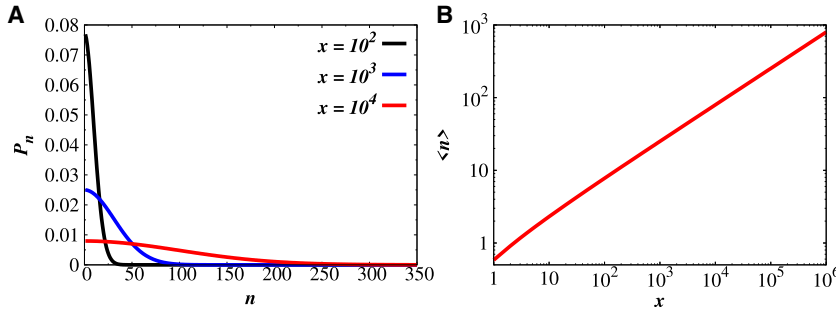


FIGURE 2 (A) Stationary distributions of holin proteins inside the membrane for different values of the coupling parameter x . (B) The average number of holins in the membrane as a function of x .

$$\Pi_0(m) = \tilde{F}_0(m, s = 0) \simeq \frac{m}{x}. \quad (\text{Equation 12})$$

We are especially interested in two other major quantities. The first one is mean first-passage times or mean lysis times, which are defined as the average times for the cell lysis to occur from the state m starting from the state $n = 0$ (no holins in the membrane). The second one is the coefficient of variation (CV) or noise in the system, which quantifies the extent of stochasticity in the holin protein expression. These properties are important since they have been measured in experiments, providing crucial quantitative insights for clarifying the molecular mechanisms of cell lysis. We explicitly calculated the average cell lysis times (for $x \gg 1$),

$$T_0(m) = - \frac{\partial \tilde{F}_0(m, s)}{\partial s} \Big|_{s=0} \simeq \frac{1+m}{k}. \quad (\text{Equation 13})$$

Similarly, we explicitly evaluated the mean-squared cell lysis times,

$$T_{02}(m) = \frac{\partial^2 \tilde{F}_0(m, s)}{\partial s^2} \Big|_{s=0} \simeq \frac{(1+m)(2+m)}{k^2}. \quad (\text{Equation 14})$$

Then, the squared CV (CV^2), or temporal noise in the system (40,41,43), is given by

$$CV^2 = \frac{T_{02}(m) - T_0(m)^2}{T_0(m)^2} \simeq \frac{1}{1+m}. \quad (\text{Equation 15})$$

RESULTS

Interplay between holin accumulation and cell lysis leads to a threshold-like dynamic behavior

One of the main features of cell lysis is an apparent threshold behavior when the membrane breaking starts only after the number of holin proteins inside the membrane reaches some specific value. Our theoretical approach can reproduce this dynamic behavior. To show this, let us define a probability that cell lysis occurs in the state n :

$$p_n = \frac{nr}{nr+k} = \frac{n}{n+x}. \quad (\text{Equation 16})$$

The physical meaning of this result is as follows. When the system is in the state n , there are two possible transitions

out of this state. One more holin protein can be added with the rate k , leading the system to the state $n+1$, or cell lysis might occur here with the rate nr . Then, the probability of cell lysis from the given state n is equal to the probability of the system to choose the lysis pathway out of this state (see Fig. 1 B). Then, one can specify the probability to have the cell lysis exactly when there are n holin proteins in the membrane as

$$Q_n = \left(\prod_{j=1}^{n-1} (1-p_j) \right) p_n. \quad (\text{Equation 17})$$

This expression can be easily understood. There are no lysis events from the states $1 \leq j \leq n-1$, each occurring with the probabilities $(1-p_j)$, and there is the lysis event from the state n , which happens with the probability p_n . This quantity is illustrated in Fig. 3 for realistic values of the coupling parameter x . One can see that there is a range of numbers of holin proteins in the membrane at which it is the most probable to observe the cell lysis. This happens close to the maximum in the protein number distribution ($n \simeq 100$ in Fig. 3). But this behavior is very similar to the existence of the threshold. Thus, we can easily associate the maximum in the distribution function Q_n with the threshold value observed in real systems. These simple arguments show that the coupling of two stochastic processes, namely increasing the number of holin proteins (with a rate

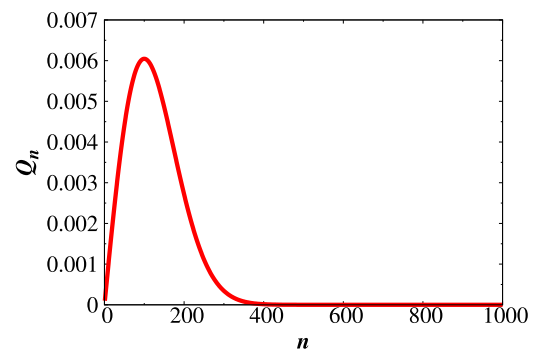


FIGURE 3 Theoretical prediction for exact distribution of holin proteins at which cell lysis occurs. The calculations are done using Eq. 17 for $x = 10^4$.

k) and decreasing the number of holins due to cell lysis (with a rate constant r), can lead to an effective threshold-like dynamics, which is consistent with experimental observations (40).

As suggested by our theoretical analysis, cell lysis occurs with the highest probability for a narrow range of holin protein numbers (close to the maximum in the distribution Q_n in Fig. 3). However, for calculations, it is convenient to choose a specific value of proteins in the membrane,

$$\bar{n} = \sum_{n=1}^{\infty} nQ_n, \quad (\text{Equation 18})$$

which can be viewed as the average number of holin proteins in the membrane that leads to cell lysis. Since this quantity closely correlates with the stationary average number of holins in the membrane, $\langle n \rangle \sim \bar{n}$, in our analysis, we associate $\langle n \rangle$ with the effective threshold that triggers cell lysis.

Cell lysis dynamics

To obtain a comprehensive description of cell lysis dynamics, the method of first-passage probabilities is employed. More specifically, we assume that the system starts in the state $n = 0$ (no holin proteins in the membrane) and the cell lysis starts from the specific state m . In our approach, we approximate the average number of holins as an effective threshold, which means that $m \simeq \langle n \rangle$. This allows us to explicitly evaluate the distributions of cell lysis times using Eq. 11.

Now we can utilize analytical predictions for cell lysis time distributions to describe all experimental observations. To fit the distribution of experimentally measured lysis times with theoretically calculated values, we utilized the raw data from (40), in which a site-directed mutagenesis approach was employed to create a repertoire of mutations in the S105 holin allele, with each mutation differing from the parent allele by one or two amino acid substitutions. These mutated sequences were employed to construct a library of lysogenic λ phages, each harboring a holin gene with slight variations. These engineered viruses were then

introduced to *E. coli* bacteria, and the induction of lysis was achieved through thermal means. The ensuing lysis events were quantified at the single-cell level, with measurements conducted for 90 – 175 bacterial cells per strain (40).

Subsequently, we performed optimal fitting of the histogram of experimental lysis time data against the theoretical predictions for both the WT holin and its 20 mutants, as illustrated in Figs. 4 and S2 (see also the supporting material for more details). Our goal was to estimate the kinetic parameters k (membrane entrance rate) and r (lysis rate constant) for each holin system, from which all dynamic properties can be explicitly calculated. Fig. 4 displays the fitting for two cases, WT and mutant JJD414, while the results for the remaining 19 mutants are presented in Fig. S2. All parameters obtained from these fittings for each holin mutant are presented in Table 1 together with all calculated dynamic quantities. We performed the goodness-of-fit analysis using the Kolmogorov-Smirnov test to assess the reliability of our parameter fitting. As presented in the supporting material, the corresponding Kolmogorov-Smirnov test statistics support the goodness of fit for all distributions (see Fig. S3 and the supporting material for details).

Dynamic properties obtained in our theoretical analysis and assembled in Table 1 provide valuable insights into the molecular mechanisms of cell lysis. One can see that the holin accumulation rate k exhibits two orders of magnitude variation from 0.03 to 3.3 min^{-1} for different species investigated in these experiments, and the corresponding rate for the WT holins is closer to the upper limit ($\sim 2.9 \text{ min}^{-1}$), but it is not the fastest one. The cell lysis rate per unit protein (r) varies only one order of magnitude from 0.69×10^{-4} to $9.4 \times 10^{-4} \text{ min}^{-1}$ for different holins, and the WT species exhibit low lysis rates, although not the slowest one. We speculate that the differences in variability of the kinetic parameters probably reflect the importance of mutations. They modify the physical-chemical properties of holin proteins, affecting their abilities to enter the membrane (k), while the effect is weaker for the lysis rates (r) because, in this case, the ability of the membrane to open holes (mutation independent) is more relevant. The coupling coefficient $x = k/r$, however, reaches the highest possible value for the WT holin proteins, providing an important clue

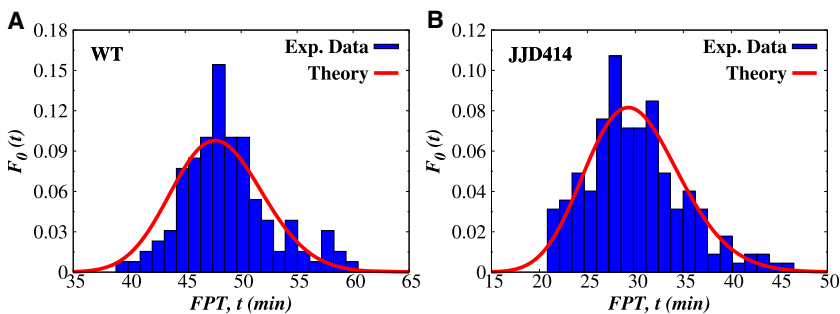


FIGURE 4 Experimental cell lysis times distributions (blue bars) fitted with our analytical predictions (red curves): (A) for WT holin proteins and (B) for mutant JJD414 holin species. The best-fitted parameters k and x are listed in Table 1 (see also the supporting material for more details).

TABLE 1 Optimized parameters for all holin mutants obtained from the best fitting of the theory to the experimental data

Sl. no.	Holin mutants	k (min^{-1})	r (min^{-1})	$x \left(= \frac{k}{r} \right)$	$\langle n \rangle$ (no. of holins)	\bar{n} (no. of holins)
1	JJD3 (WT)	2.9	0.96×10^{-4}	30×10^3	138	218
2	JJD5 (S105)	1.7	1.9×10^{-4}	9.1×10^3	76	120
3	JJD246	1.7	1.3×10^{-4}	13×10^3	90	142
4	JJD248	1.8	2.1×10^{-4}	8.7×10^3	74	117
5	JJD251	1.7	5.8×10^{-4}	2.9×10^3	43	68
6	JJD253	2.0	5.0×10^{-4}	3.9×10^3	50	79
7	JJD388	0.06	4.6×10^{-4}	0.14×10^3	9	15
8	JJD389	0.03	6.0×10^{-4}	0.05×10^3	5	9
9	JJD390	0.24	1.5×10^{-4}	1.6×10^3	31	50
10	JJD391	0.3	1.7×10^{-4}	1.5×10^3	30	48
11	JJD404	3.1	9.4×10^{-4}	3.3×10^3	46	73
12	JJD405	3.3	7.0×10^{-4}	4.7×10^3	54	86
13	JJD411	0.08	4.5×10^{-4}	0.19×10^3	11	17
14	JJD413	3.0	5.1×10^{-4}	5.9×10^3	61	96
15	JJD414	1.3	6.1×10^{-4}	2.1×10^3	36	57
16	JJD415	1.1	7.7×10^{-4}	1.4×10^3	30	47
17	JJD426	0.2	1.9×10^{-4}	1.1×10^3	26	42
18	JJD428	0.7	1.5×10^{-4}	4.5×10^3	53	85
19	JJD432	1.1	0.69×10^{-4}	15.9×10^3	100	158
20	JJD434	1.4	0.89×10^{-4}	15.3×10^3	98	155
21	JJD436	1.2	0.72×10^{-4}	16.1×10^3	101	160

about how cell lysis processes are regulated in nature. It is almost 1000 times larger ($x \approx 0.05 \times 10^3$) than that for the mutant JJD389 and twice as large ($x \approx 16.1 \times 10^3$) as that for the mutant JJD436, which shows the closest value of the coupling parameter.

An important result of our theoretical analysis presented in Table 1 is the ability to estimate the number of holin proteins in the membrane when cell lysis occurs. We predict that for the WT system, the number of accumulated holins in the membrane before the lysis will be in the order of 140 – 220 molecules. This is consistent with experimentally measured numbers of S105 holin molecules for lysis, obtained from quantitative Western blotting, that show a broad range, spanning from as many as 1000 to as few as 50 molecules (33). Importantly, for all investigated mutants, the number of accumulated holin proteins is always smaller, reaching as low as only 5 – 10 molecules for the mutant JJD389. This wide range of protein numbers needed to trigger cell lysis supports our assumption that lysis can, in principle, occur for any number of holins in the membrane. The balance between holin accumulations and holin removal due to cell lysis determines the specific range at which the inner membrane can be broken with the highest probability. We also note that the predicted stationary average number of holin proteins ($\langle n \rangle$) and the average number before cell lysis (\bar{n}) are not the same quantities, but they strongly correlate. Our analysis suggests that $\bar{n}/\langle n \rangle \sim 1.6$ for all studied holin systems (for more details, see Fig. S4). This also means that it does not matter what quantity is chosen as an effective threshold as long as only one of them is utilized. In our calculations,

we selected $\langle n \rangle$ as an effective threshold for analyzing all WT and mutant species.

Noise in lysis timing

One of the most intriguing observations from Table 1 is the distinctive behavior of WT holins from all other mutant species that exhibit the strongest coupling and the largest number of proteins before the lysis event. To better understand the underlying mechanisms, we evaluated the noise in different holin systems and compared it with experimentally measured values. The results are presented in Fig. 5, where the coefficients of variance are explicitly calculated for different holin species. One can see (Fig. 5 A) that increasing the number of holins in the membrane lowers the noise in cell lysis times, and the smallest noise is observed for the WT species. This decreasing trend in CV^2 as the function of the average number of accumulated holin proteins perfectly agrees with experimental data (40), and it is also consistent with previous theoretical observations (17,41). Although the molecular mechanisms of noise reduction with an increase in the number of accumulated holin proteins are still not clear, we might speculate that for the larger number of protein molecules, there are more ways to cooperatively aggregate and open the holes in the membrane, leading to more precise timing in cell lysis events.

It is interesting to note that while WT holins achieve the lowest level of temporal noise, they are not the fastest in cell lysis dynamics. One can see this in Fig. 5 B, where the non-monotonic behavior of CV^2 as a function of the mean lysis times is observed. Several holin mutant species produce

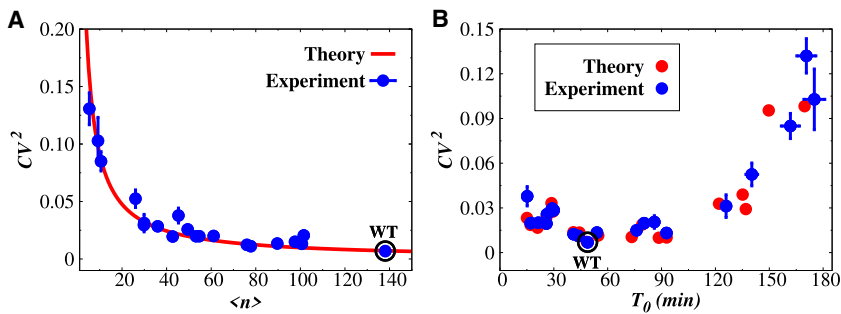


FIGURE 5 (A) Temporal noise in cell lysis times as a function of the average number of holin proteins in the membrane. Theoretical predictions of CV^2 are given by the red line, and experimental observations (from (40)) are represented by blue symbols. (B) Temporal noise in cell lysis times as a function of the mean cell lysis times. Theoretical predictions of CV^2 are given by red symbols, and experimental observations (from (40)) are represented by blue symbols. Each data point corresponds to different WT and mutant species. The result for the WT holin protein is highlighted by the black circle. Error bars are 95% confidence intervals, obtained after bootstrapping of 1000 replicas (see the [supporting material](#) for more details).

faster cell lysis events, but all of them exhibit larger noise. These observations can be explained in the following way. It takes time to accumulate holin proteins before they can break the membrane, and the corresponding temporal noise is smaller. This is the case for WT species. However, for some mutants, cell lysis can occur for the smaller number of accumulated protein molecules. This leads to fast cell lysis times, as observed in Fig. 5 B, but simultaneously, due to a smaller number of proteins, these systems exhibit significant fluctuations.

To better understand the microscopic details of cell lysis dynamics, we also evaluated the spatial distributions of holin proteins and performed a bootstrapping analysis, which is a resampling technique that involves drawing multiple random samples with replacements from the original dataset of the experimental lysis times of each mutant (see the [supporting material](#) for more details). The results are illustrated in Fig. 6. For each bootstrap iteration, a subset of the data was randomly selected, and the corresponding histogram was computed. Subsequently, the average number of accumulated holin proteins was optimized to best fit the observed histogram with our theoretical predictions using the “Nelder-Mead” optimization method (49,50). This process was repeated over a specified number of bootstrap samples (1000 iterations in our case), resulting in a distribution of the optimized parameters (see Figs. 6 A for WT and B, and S5 for all other holin mutants). From these distributions, we calculated the mean values and constructed error bars in the form of a confidence interval. The confidence interval, set at a 95% level, was determined by computing the 2.5th and 97.5th percentiles of the bootstrapped n values. The resulting mean values ($\langle n \rangle$) for each of the holin mutants and their associated error bars are shown in Fig. 6 C.

Now one can see from Fig. 6 what additional features distinguish different holin proteins in their abilities to break the membrane. WT holins accumulate the largest number of proteins before cell lysis events, and this system is also characterized by a very narrow spatial distribution of proteins around the mean number $\langle n \rangle$ (Fig. 6 A). Our calculations suggest strong correlations between temporal and spatial noise, as indicated in Fig. S6. This explains why WT holins exhibit precise timing in cell lysis. The situation is very

different for mutant species. Most of them show broad spatial distributions that lead to significant levels of noise in cell lysis dynamics (Figs. 6, B, C, and S5). There are a few mutant species (e.g., JJD388 and JJD389) that also have relatively narrow distributions of accumulated proteins inside the membranes. But in these systems, the membrane breaking occurs when the number of proteins is small, and this leads to significant fluctuations in cell lysis times. Thus, this analysis allows us to explore the proposed theoretical model for capturing the dynamics of holin-mediated cell lysis, providing valuable insights into the possible molecular mechanisms.

DISCUSSION

A large number of biological processes exhibit surprising temporal precision of underlying events despite relying on underlying stochastic transitions. These processes are frequently associated with threshold-like behavior when reaching the specific concentration of regulatory proteins triggering the event. At the same time, there is a significant gap in our understanding of the molecular mechanisms of such precise timing because most theoretical studies do not explain the appearance of thresholds. In this paper, we attempted to provide a possible microscopic picture of how biological systems can achieve remarkable, almost deterministic accuracy and robustness in their performance. We hypothesize that this is a result of the coupling of underlying stochastic processes that might lead to the cancellation of noise.

To test our idea, we concentrated on investigating precise timing in cell lysis when holin proteins produced by virus-hijacked cell machinery break the inner membranes of gram-negative bacteria. The main reason for studying cell lysis is the large amount of quantitative data obtained for both WT and various mutant species that allow for comprehensive testing of theoretical ideas. For this purpose, we introduced a minimal stochastic model that takes into account the most relevant physical-chemical processes, such as protein accumulation inside the membrane and membrane breaking that leads to the loss of holin proteins. It is shown that coupling these two processes leads to effective threshold-like dynamics in the system. This is

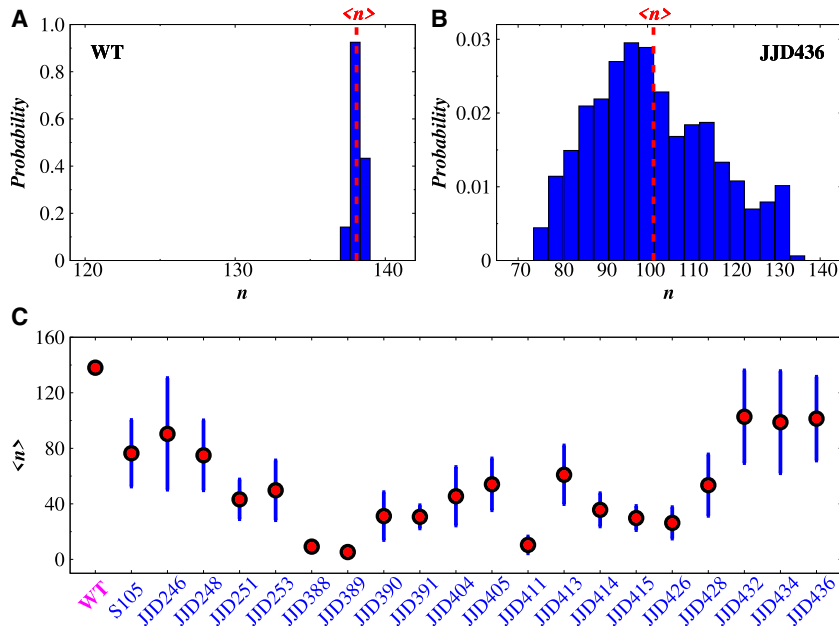


FIGURE 6 (A) Spatial distribution of holin proteins in WT species. (B) Spatial distribution of holin proteins in the mutant JJD436 species. The red dashed line corresponds to the average holin numbers $\langle n \rangle$. (C) Variation in the average number of holins for triggering cell lysis for all mutants obtained from the bootstrapping analysis. Error bars represent 95% bootstrap confidence interval.

because increasing the number of holin proteins in the membrane is balanced by their removal during cell lysis events. If the number of holin proteins in the membrane is small, then the cell lysis is not happening because the corresponding rates are low. If the number of holin proteins is large, then such systems have a low probability of existence because of very fast rates of cell lysis. As a result, there is a narrow range of protein concentrations in the membrane at which cell lysis can be observed, and this exactly corresponds to thresholds observed in real biological systems.

After showing that our stochastic model can reproduce the threshold behavior, we solved the model exactly, allowing us to obtain all the dynamic properties of the process. Then, applying this theoretical framework for experimental observations on WT and mutant holin proteins, we were able to extract the relevant kinetic parameters, leading to a comprehensive description of cell lysis dynamics. This analysis allowed us to better understand the molecular picture of precise timing in cell lysis. It is found that this is the result of the fact that the WT systems are trying to accumulate as many holin proteins as possible in the membrane before cell lysis. In addition, nature tunes the spatial distribution of accumulated proteins inside the membrane to be quite narrow. The large number of available holins and the narrow spatial distribution lead to very low levels of temporal noise and high precision in breaking the inner membranes. For all mutant species, one or both of these conditions are not satisfied, producing systems with large temporal fluctuation in the cell lysis times.

Our theoretical analysis also suggests that there is a trade-off between the precision and speed of cell lysis. It seems that the WT systems are optimized to have low noise but not the

fastest cell lysis dynamics. Several mutants exhibit faster times to break the membrane, but simultaneously, they are quite noisy. Our theoretical calculations indicate that for the WT system, this is a result of accumulating the largest possible number of holin proteins with narrow spatial distributions inside the membrane before starting the lysis. At the same time, the system is not trying to increase the precision further by adding more holin proteins to the membrane because it eventually slows down the overall process too much to be coupled with other processes in viral reproduction. Thus, it seems that nature optimized cell lysis for λ bacteriophages to achieve the highest possible temporal precision while keeping the tolerable speeds of the process.

A fundamental aspect of "time accuracy" in biological processes is its requirement for free energy dissipation. In other words, higher temporal precision can be achieved only with additional energy dissipation, emphasizing the nonequilibrium nature of these phenomena. This aspect of precise timing has been discussed extensively in the biophysics literature. For instance, Li et al. explored kinetic timing mechanisms that improve the accuracy of GTPase timers in biological processes (51). Tu et al. investigated nonequilibrium mechanisms for ultrasensitivity in biological switches, highlighting the role of nonequilibrium conditions in achieving precise timing (52). Furthermore, Wang et al. analyzed the concurrent fast and slow cycling of proteins on gene promoters, reconciling this behavior through nonequilibrium physics (53). Moreover, Ray et al. provided a general expression for the dispersion of time spent in a state for unicyclic models, emphasizing dissipation-less precision in timing (54). All these studies underscore the importance of nonequilibrium dynamics in achieving precise temporal regulation in biological systems.

In our study, we also observed that precise timing in holin-mediated cell lysis is the result of nonequilibrium processes. The accumulation and subsequent removal of holin proteins are processes that involve energy dissipation. The trade-off between precision and speed, as well as the requirement for narrow spatial distributions of holin proteins, suggest that the system operates far from equilibrium to maintain high temporal accuracy. This is consistent with the broader understanding that biological systems dissipate energy to achieve and regulate temporal precision. Thus, our model aligns with the concept that free energy dissipation is crucial for the precise timing of cell lysis, reinforcing the idea that such nonequilibrium processes are fundamental for achieving the observed deterministic behavior in biological systems. Furthermore, our discrete-state stochastic approach seems to be convenient for explicit calculations of energy dissipation, and we plan to do it soon.

While our theoretical approach presents a plausible physical-chemical picture to explain the almost deterministic dynamic behavior of biological processes with high temporal precision, as illustrated for cell lysis phenomena, it is important to discuss its limitations. The utilized theoretical model of cell lysis is rather overly simplified because it essentially considers only two processes, protein accumulation and protein removal, lumping together multiple biochemical and biophysical transformations. In real systems, many other important transitions occur. Taking them into account might influence our quantitative predictions, but one expects that the main physical conclusions should not be affected. Our main criticism of current theoretical methods is their assumptions of specific thresholds without explaining their origin. While we presented a possible microscopic picture of how the threshold-like behavior appears and found a distribution of threshold values, in our specific calculations, we utilized a single value of the threshold (average number of holin proteins). A better theoretical analysis should account for such distributions more quantitatively. Our theoretical approach also does not consider possible mechano-chemical changes in the membranes due to the accumulation of holin proteins inside of them. Furthermore, the analysis assumes that the system quickly reaches the stationary state, which might not be always the case. However, despite these considerations, the proposed theoretical framework provides physically clear mechanisms of possible noise reduction during the dynamic regulation of biological processes. Its main advantage is the ability to present a fully quantitative description that explains existing experiments and can be explicitly tested in future experiments. It also clarifies many important molecular aspects of dynamic regulation in biological phenomena.

SUPPORTING MATERIAL

Supporting material can be found online at <https://doi.org/10.1016/j.bpj.2024.07.008>.

AUTHOR CONTRIBUTIONS

A.M. and A.B.K. designed research; A.M. performed research; A.M., H.T., and A.B.K. analyzed data; and A.M., H.T., and A.B.K. wrote the paper.

ACKNOWLEDGMENTS

The work was supported by the Welch Foundation (C-1559), the NIH (R01GM148537 and R01HL157714-04), the NSF (CHE-2246878), and the Center for Theoretical Biological Physics sponsored by the NSF (PHY-2019745).

DECLARATION OF INTERESTS

The authors declare no competing interests.

REFERENCES

1. Champlin, D. T., and J. W. Truman. 1998. Ecdysteroid control of cell proliferation during optic lobe neurogenesis in the moth *Manduca sexta*. *Development*. 125:269–277.
2. Alvarado, A. S., and S. Yamanaka. 2014. Rethinking differentiation: stem cells, regeneration, and plasticity. *Cell*. 157:110–119.
3. Brun-Usan, M., C. Thies, and R. A. Watson. 2020. How to fit in: The learning principles of cell differentiation. *PLoS Comput. Biol.* 16:e1006811.
4. Piggot, P. J., and D. W. Hilbert. 2004. Sporulation of *Bacillus subtilis*. *Curr. Opin. Microbiol.* 7:579–586.
5. Koopman, N., L. Remijas, ..., S. Brul. 2022. Mechanisms and applications of bacterial sporulation and germination in the intestine. *Int. J. Mol. Sci.* 23:3405.
6. Bean, J. M., E. D. Siggia, and F. R. Cross. 2006. Coherence and timing of cell cycle start examined at single-cell resolution. *Mol. Cell*. 21:3–14.
7. Chen, K. C., L. Calzone, ..., J. J. Tyson. 2004. Integrative analysis of cell cycle control in budding yeast. *Mol. Biol. Cell*. 15:3841–3862.
8. Basu, S., J. Greenwood, ..., P. Nurse. 2022. Core control principles of the eukaryotic cell cycle. *Nature*. 607:381–386.
9. Goldschmidt, Y., E. Yurkovsky, ..., I. Nachman. 2015. Control of relative timing and stoichiometry by a master regulator. *PLoS One*. 10:e0127339.
10. Negrete, J., and A. C. Oates. 2021. Towards a physical understanding of developmental patterning. *Nat. Rev. Genet.* 22:518–531.
11. Pedraza, J. M., and J. Paulsson. 2007. Random timing in signaling cascades. *Mol. Syst. Biol.* 3:81.
12. McAdams, H. H., and A. Arkin. 1997. Stochastic mechanisms in gene expression. *Proc. Natl. Acad. Sci. USA*. 94:814–819.
13. Co, A. D., M. C. Lagomarsino, ..., M. Osella. 2017. Stochastic timing in gene expression for simple regulatory strategies. *Nucleic Acids Res.* 45:1069–1078.
14. Teimouri, H., R. Mukherjee, and A. B. Kolomeisky. 2020. Stochastic mechanisms of cell-size regulation in bacteria. *J. Phys. Chem. Lett.* 11:8777–8782.
15. Amir, A. 2014. Cell size regulation in bacteria. *Phys. Rev. Lett.* 112:208102.
16. Lloyd, A. C. 2013. The regulation of cell size. *Cell*. 154:1194–1205.
17. Ghusinga, K. R., J. J. Dennehy, and A. Singh. 2017. First-passage time approach to controlling noise in the timing of intracellular events. *Proc. Natl. Acad. Sci. USA*. 114:693–698.
18. Eldar, A., and M. B. Elowitz. 2010. Functional roles for noise in genetic circuits. *Nature*. 467:167–173.

19. Raser, J. M., and E. K. O'Shea. 2005. Noise in gene expression: origins, consequences, and control. *Science*. 309:2010–2013.
20. Tsimring, L. S. 2014. Noise in biology. *Rep. Prog. Phys.* 77:026601.
21. Briat, C., and M. Khammash. 2023. Noise in Biomolecular Systems: Modeling, Analysis, and Control Implications. *Annu. Rev. Control Robot. Auton. Syst.* 6:283–311.
22. Eling, N., M. D. Morgan, and J. C. Marioni. 2019. Challenges in measuring and understanding biological noise. *Nat. Rev. Genet.* 20:536–548.
23. Wang, I. N., D. L. Smith, and R. Young. 2000. Holins: the protein clocks of bacteriophage infections. *Annu. Rev. Microbiol.* 54:799–825.
24. Golding, I. 2018. Infection by bacteriophage lambda: an evolving paradigm for cellular individuality. *Curr. Opin. Microbiol.* 43:9–13.
25. Gründling, A., U. Bläsi, ..., R. Young. 2000. Biochemical and genetic evidence for three transmembrane domains in the class I holin, λ S. *J. Biol. Chem.* 275:769–776.
26. Gründling, A., M. D. Manson, ..., R. Young. 2001. Holins kill without warning. *Proc. Natl. Acad. Sci. USA.* 98:9348–9352.
27. Dewey, J. S., C. G. Savva, ..., R. Young. 2010. Micron-scale holes terminate the phage infection cycle. *Proc. Natl. Acad. Sci. USA.* 107:2219–2223.
28. Summer, E. J., J. Berry, ..., R. Young. 2007. Rz/Rz1 lysis gene equivalents in phages of Gram-negative hosts. *J. Mol. Biol.* 373:1098–1112.
29. Berry, J., E. J. Summer, ..., R. Young. 2008. The final step in the phage infection cycle: the Rz and Rz1 lysis proteins link the inner and outer membranes. *Mol. Microbiol.* 70:341–351.
30. Young, R. 2013. Phage lysis: do we have the hole story yet? *Curr. Opin. Microbiol.* 16:790–797.
31. Young, R. 2014. Phage lysis: three steps, three choices, one outcome. *J. Microbiol.* 52:243–258.
32. Rajaure, M., J. Berry, ..., R. Young. 2015. Membrane fusion during phage lysis. *Proc. Natl. Acad. Sci. USA.* 112:5497–5502.
33. White, R., S. Chiba, ..., R. Young. 2011. Holin triggering in real time. *Proc. Natl. Acad. Sci. USA.* 108:798–803.
34. Park, T., D. K. Struck, ..., R. Young. 2006. Topological dynamics of holins in programmed bacterial lysis. *Proc. Natl. Acad. Sci. USA.* 103:19713–19718.
35. Raab, R., G. Neal, ..., R. Young. 1986. Mutational analysis of bacteriophage lambda lysis gene S. *J. Bacteriol.* 167:1035–1042.
36. Pang, T., T. Park, and R. Young. 2010. Mutational analysis of the S21 pinholin. *Mol. Microbiol.* 76:68–77.
37. Ramanculov, E., and R. Young. 2001. Genetic analysis of the T4 holin: timing and topology. *Gene.* 265:25–36.
38. Dennehy, J. J., and I. N. Wang. 2011. Factors influencing lysis time stochasticity in bacteriophage λ . *BMC Microbiol.* 11:174.
39. To, K. H., and R. Young. 2014. Probing the structure of the S105 hole. *J. Bacteriol.* 196:3683–3689.
40. Kannoly, S., T. Gao, ..., J. J. Dennehy. 2020. Optimum threshold minimizes noise in timing of intracellular events. *iScience.* 23:101186.
41. Singh, A., and J. J. Dennehy. 2014. Stochastic holin expression can account for lysis time variation in the bacteriophage λ . *J. R. Soc. Interface.* 11:20140140.
42. Rijal, K., A. Prasad, and D. Das. 2020. Protein hourglass: Exact first passage time distributions for protein thresholds. *Phys. Rev. E.* 102:052413.
43. Rijal, K., A. Prasad, ..., D. Das. 2022. Exact distribution of threshold crossing times for protein concentrations: Implication for biological timekeeping. *Phys. Rev. Lett.* 128:048101.
44. Wong, F., and A. Amir. 2019. Mechanics and dynamics of bacterial cell lysis. *Biophys. J.* 116:2378–2389.
45. Gründling, A., D. L. Smith, ..., R. Young. 2000. Dimerization between the holin and holin inhibitor of phage λ . *J. Bacteriol.* 182:6075–6081.
46. White, R., T. A. Tran, ..., R. Young. 2010. The N-terminal transmembrane domain of λ S is required for holin but not antiholin function. *J. Bacteriol.* 192:725–733.
47. Kolomeisky, A. B. 2015. Motor Proteins and Molecular Motors. CRC Press, Boca Raton, FL.
48. Redner, S. 2001. A Guide to First-Passage Processes. Cambridge University Press, Cambridge, UK.
49. Virtanen, P., R. Gommers, ..., Y. Vázquez-Baeza. 2020. SciPy 1.0: Fundamental algorithms for scientific computing in Python. *Nat. Methods.* 17:261–272.
50. Nelder, J. A., and R. Mead. 1965. A simplex method for function minimization. *Comput. J.* 7:308–313.
51. Li, G., and H. Qian. 2002. Kinetic timing: a novel mechanism that improves the accuracy of GTPase timers in endosome fusion and other biological processes. *Traffic.* 3:249–255.
52. Tu, Y. 2008. The nonequilibrium mechanism for ultrasensitivity in a biological switch: sensing by Maxwell's demons. *Proc. Natl. Acad. Sci. USA.* 105:11737–11741.
53. Wang, Y., F. Liu, ..., W. Wang. 2014. Reconciling the concurrent fast and slow cycling of proteins on gene promoters. *J. R. Soc. Interface.* 11:20140253.
54. Ray, S., and A. C. B. 2017. Dispersion of the time spent in a state: general expression for unicyclic model and dissipation-less precision. *J. Phys. Math. Theor.* 50:355001.